Bioorganic & Medicinal Chemistry xxx (2010) xxx–xxx

Contents lists available at ScienceDirect

Bioorganic & Medicinal Chemistry

journal homepage: www.elsevier.com/locate/bmc

Inhibition of *Mycobacterium tuberculosis* tyrosine phosphatase PtpA by synthetic chalcones: Kinetics, molecular modeling, toxicity and effect on growth

Alessandra Mascarello [a], Louise Domeneghini Chiaradia [a], Javier Vernal [b,c], Andrea Villarino [f], Rafael V. C. Guido [d], Paulo Perizzolo [e], Valerie Poirier [e], Dennis Wong [e], Priscila Graziela Alves Martins [b,c], Ricardo José Nunes [a], Rosendo Augusto Yunes [a], Adriano Defini Andricopulo [d], Yossef Av-Gay [e,*], Hernán Terenzi [b,c,*]

[a] *Laboratório Estrutura e Atividade, Departamento de Química, LEAT-CFM-UFSC, Universidade Federal de Santa Catarina, Campus Trindade, 88040-900 Florianópolis, SC, Brazil*
[b] *Centro de Biologia Molecular Estrutural, Departamento de Bioquímica, CEBIME-UFSC, Universidade Federal de Santa Catarina, Campus Trindade, 88040-900, Florianópolis, SC, Brazil*
[c] *INBEB-CNPq (Instituto Nacional de Ciência e Tecnologia de Biologia Estrutural e Bioimagem), Universidade Federal do Rio de Janeiro, Rio de Janeiro, RJ 21941-590, Brazil*
[d] *Laboratório de Química Medicinal e Computacional, Instituto de Física de São Carlos, LQMC-IFSC-USP, Universidade de São Paulo, 13566-590 São Carlos, SP, Brazil*
[e] *Department of Medicine, Division of Infectious Diseases, University of British Columbia, Vancouver, British Columbia, Canada*
[f] *Institut Pasteur de Montevideo, CP 11400, Montevideo, Uruguay*

ARTICLE INFO

Article history:
Received 17 February 2010
Revised 15 April 2010
Accepted 17 April 2010
Available online xxxx

Keywords:
Tuberculosis
Tyrosine phosphatase inhibitors
Chalcones

ABSTRACT

Tuberculosis (TB) is a major cause of morbidity and mortality throughout the world, and it is estimated that one-third of the world's population is infected with *Mycobacterium tuberculosis*. Among a series of tested compounds, we have recently identified five synthetic chalcones which inhibit the activity of *M. tuberculosis* protein tyrosine phosphatase A (PtpA), an enzyme associated with *M. tuberculosis* infectivity. Kinetic studies demonstrated that these compounds are reversible competitive inhibitors. In this work we also carried out the analysis of the molecular recognition of these inhibitors on their macromolecular target, PtpA, through molecular modeling. We observed that the predominant determinants responsible for the inhibitory activity of the chalcones are the positions of the two methoxyl groups at the A-ring, that establish hydrogen bonds with the amino acid residues Arg17, His49, and Thr12 in the active site of PtpA, and the substitution of the phenyl ring for a 2-naphthyl group as B-ring, that undergoes π stacking hydrophobic interaction with the Trp48 residue from PtpA. Interestingly, reduction of mycobacterial survival in human macrophages upon inhibitor treatment suggests their potential use as novel therapeutics. The biological activity, synthetic versatility, and low cost are clear advantages of this new class of potential tuberculostatic agents.

1. Introduction

Tuberculosis is an infection of the human respiratory tract caused by *Mycobacterium tuberculosis* (Mtb) and according to the last report of WHO, it is estimated that this disease provokes about two million deaths each year.[1] The past two decades have seen a decline in the effectiveness of the present regimen of TB drugs as a result of both the mutation of *M. tuberculosis*, in response to selective pressure, and evolving demographics of patients population, including co-infection with HIV, and the growing type-2 diabetes epidemic, that should not be ignored. Consequently, a new TB drug will not only have to pass all the safety requirements associated with prolonged administration but also has to be compatible with antiretroviral therapy and, possibly, other medications.[2–4]

In the past decade many advances in the understanding of metabolic and intracellular processes of Mtb have been achieved, helped by the publication of its complete genome sequence.[5] The virulence of this microorganism is clearly associated with its mechanism of host cellular invasion, and also signal transduction events between the bacteria and the macrophages are essential for its survival in vivo.[6–8]

The analysis of Mtb genome indicated the presence of genes coding for protein tyrosine phosphatases (PTP) MPtpA and MPtpB.[5] Despite the absence of any known export signal, these two enzymes are secreted by mycobacteria and involved in survival in host macrophages.[7–9] The primary function of these protein tyrosine phosphatases (PTPs) may be to modulate tyrosine-phosphorylated host proteins. Confirming this assumption, we have shown that PtpA inactivation attenuates the growth of Mtb in human macrophages, and more interestingly, the macrophage protein target, the vacuolar protein sorting 33 homolog B (VPS33B), a regulator of membrane fusion, is a substrate of this enzyme.[10] Inhibition

* Corresponding authors. Tel.: +55 48 3721 6426; fax: +55 48 3721 9672.
E-mail addresses: yossi@interchange.ubc.ca (Y. Av-Gay), hterenzi@ccb.ufsc.br (H. Terenzi).

0968-0896/$ - see front matter © 2010 Elsevier Ltd. All rights reserved.
doi:10.1016/j.bmc.2010.04.051

of VPS33B activity leads to phagosome–lysosome fusion, a cellular response to infection process, blocked by Mtb infection.[10]

More recently, the presence of a phosphotyrosine kinase, PtkA, was detected in Mtb, and interestingly PtpA was shown to be a substrate of PtkA, although PtkA is not a substrate for PtpA.[11] To survive in humans, pathogenic bacteria have evolved many mechanisms to evade the host immune response.[9–12] Protein phosphatases are virulence factors in infectious diseases caused by *Yersinia pestis*, *Salmonella typhimurium*, and *M. tuberculosis*.[13] Low-molecular-weight tyrosine phosphatases are secreted by pathogenic bacteria, and MPtpA is an example that was shown to be required for growth of *M. tuberculosis* in human macrophages.[10] Thus, inhibition of PtpA activity may modulate mycobacteria survival inside macrophages.

Among the pioneers in the description of PtpA inhibitory compounds Waldmann and co-workers[14,15] tested natural products such as stevastelins, roseophilins and prodigiosins, obtaining IC_{50} values between 8.8 μM and 28.7 μM. Madhurantakam et al. identified as reversible inhibitors of MPtpA, the phosphate analogs molibdate, orthovanadate and sodium tungstate, with IC_{50} values of 24.5 μM, 28.0 μM, and 30.8 μM, respectively.[16] More recently, one aryl difluoromethylphosphonic acid compound was identified as a potent inhibitor of PtpA, with K_i value of 1.4 ± 0.3 μM.[17]

Although few natural products have been identified as PTP inhibitors, the major strategy that has been adopted is the design of small molecules based on nonhydrolyzable phosphotyrosine analogs.[18] Searching for selective inhibitors for MPtpB, one interesting compound (oxalylamino-methylene)-thiophene sulfonamide (OMTS), with an IC_{50} value of 0.44 μM was described, with high specificity and selectivity for PtpB.[19] Recently, Waldmann's group used BIOS (Biology-Oriented Synthesis) to obtain a series of indolo [2,3-α]quinolizidines as inhibitors of MPtpB.[20]

One important criterion for compound collections for applications in chemical biology and research in medicinal chemistry is their relevance to nature.[21] The structural scaffolds of natural products can be recognized for binding to proteins and, therefore, have biological relevance.[18] Based on this late assumption, chalcones, which are precursors of flavonoids in plants, appear as promising lead compounds in the search of new inhibitors of PTPs. In particular, naphthylchalcones seem to be interesting, because biphenyl- and naphthyl-substituted compounds show higher potency than phenyl derivatives, due to hydrophobic interactions playing a dominant role in the stabilization of inhibitor–enzyme interactions.[22]

The important advances in genomic and proteomic, as well as the evolution of X-ray crystallography and Nuclear Magnetic Resonance (NMR), provided a significant increase in the number of molecular targets that are available as 3D structures in Protein Data Bank (PDB).[23] The knowledge of the structure of the macromolecular target allows the rational planning of enzymatic inhibitors through Structure Based Drug Design (SBDD). Molecular docking is one of the main methods of SBDD used in medicinal chemistry, and have been contributing significantly in the optimization of lead compounds, adjusting power, affinity and pharmacokinetic properties.[24]

Part of our research program aimed at discovering novel MPtpA inhibitors and in order to identify the mechanism of action of the inhibitors, we have evaluated a small library of chalcones derivatives.[25] In the present work lead compounds were available from previous results from our group,[25] and we aimed at understanding the molecular mechanism responsible for the inhibition of MPtpA and also for guiding selectivity. In this report, we analyze the mechanism of PtpA inhibition mediated by active chalcones, using molecular modeling, enzyme kinetics analysis, and in vivo activity and toxicity of the five most potent chalcone inhibitors of MPtpA.

2. Results and discussion

Chalcones are essential intermediate compounds in flavonoid biosynthesis in plants, and present many biological entities,[26,27] including those described against *M. tuberculosis*.[28a] Recently, licochalcone A derivatives were identified as inhibitors of human PTP1B.[28b] Also, Chibale and co-workers reviewed the use of chalcones as antitubercular agents inhibiting phosphatases.[28c]

Chalcones are essential intermediate compounds in flavonoid biosynthesis in plants, and present many biological entities,[26,27] including those described against *M. tuberculosis*.[28] Previous results from our group[25] indicated that from 38 synthetic chalcones assayed, five were low micromolar inhibitors of the PtpA from Mtb: **5i** (IC_{50} = 53.7 ± 1.3 μM); **4d** (IC_{50} = 50.2 ± 2.1 μM); **4a** (IC_{50} = 39.5 ± 1.1 μM); **5j** (IC_{50} = 23.1 ± 1.6 μM); **5a** (IC_{50} = 8.4 ± 0.9 μM); these structures are presented in Figure 1.

2.1. Kinetic mechanism of inhibition

The five most potent chalcone derivatives against PtpA, were selected for further enzyme kinetics studies. The kinetic mechanism of inhibition and K_i values were determined. The results shown in Table 1 and Figure 2 indicate that the compounds exhibit competitive inhibition with respect to the substrate *p*-nitrophenyl phosphate (pNPP). The Lineweaver–Burk double-reciprocal plot (Fig. 2) shows intercepts of all lines (obtained at least with three different inhibitor concentrations) converging at the *y*-axis ($1/V_{max}$), whereas the slope (K_{mapp}/V_{max}) and *x*-axis intercepts ($-1/K_{mapp}$) vary with inhibitor concentration. In this context, the V_{max} value remains constant, and the apparent K_m values increase with increasing inhibitor concentrations. This behavior is consistent with a mutually exclusive binding mode, where the bioactive molecules compete with the substrate for the free enzyme active site.[29] The K_i values obtained for the competitive inhibitors **5i**, **4d**, **4a**, **5j**, and **5a** are in the low micromolar range (~18 μM, ~9 μM, ~21 μM; ~5 μM, and ~5 μM, respectively), indicating that the chalcone derivatives represent a new chemical diversity for the target enzyme.

2.2. Molecular modeling

Structure-based molecular docking simulations were performed in order to investigate the binding mode of the competitive inhibitors into the PtpA active site, as well as to shed light on the SAR underlying the inhibitory potency of these compounds. The binding mode of the chalcone derivatives was generated using the top-ranked poses obtained by the FlexX scoring function.[30]

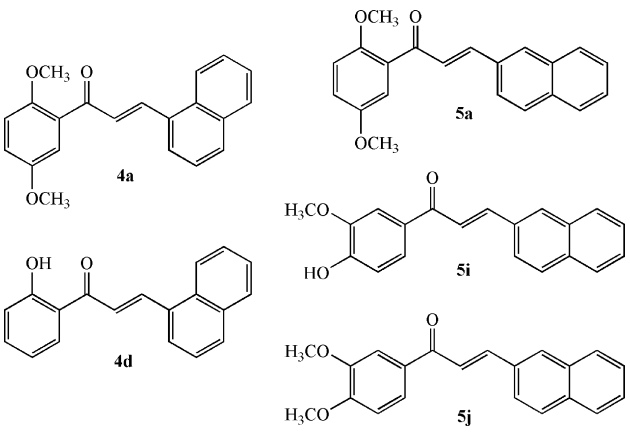

Figure 1. Molecular structure of the chalcone analogs used in this work.

Table 1
Structure and K_i values of the chalcones **4a**, **5j**, **5a**, **5i** and **4d** as MPtpA inhibitors

Compound	K_i (μM)
4a	21.3 ± 2.6
5j	4.9 ± 1.0
5a	5.4 ± 1.4
5i	17.9 ± 2.9
4d	9.1 ± 1.6

The best orientation of the inhibitors **4a** (magenta), **4d** (blue), **5a** (cyan), and **5j** (yellow) into the PtpA binding site is individually shown in Figure 3.

The dimethoxy substituted A-ring of four of the bioactive compounds is oriented towards the phosphate-binding pocket of the PtpA active site (Fig. 3). In this conformation, the *o*-methoxy and the *m*-methoxy groups of **4a** and **5a** (K_i = 21 μM and 5.4 μM, respectively) are positioned in a favorable orientation to accept

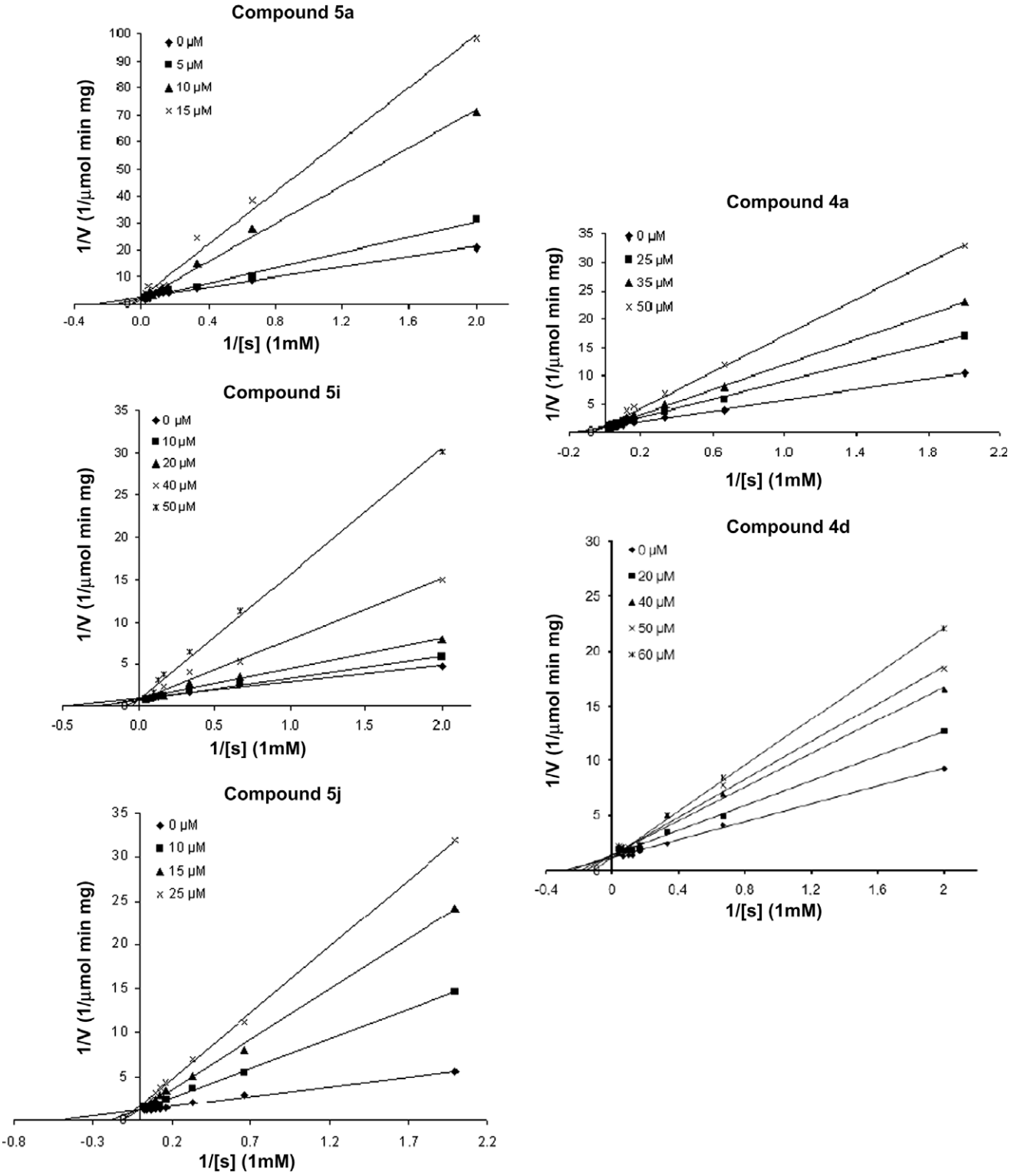

Figure 2. Competitive inhibition profile of compounds **4a**, **5j**, **5a**, **5i** and **4d**. Kinetic experiments were conducted in the presence of increasing concentrations of the inhibitors. pNPP was used as substrate in all experiments.

Please cite this article in press as: Mascarello, A.; et al. *Bioorg. Med. Chem.* (2010), doi:10.1016/j.bmc.2010.04.051

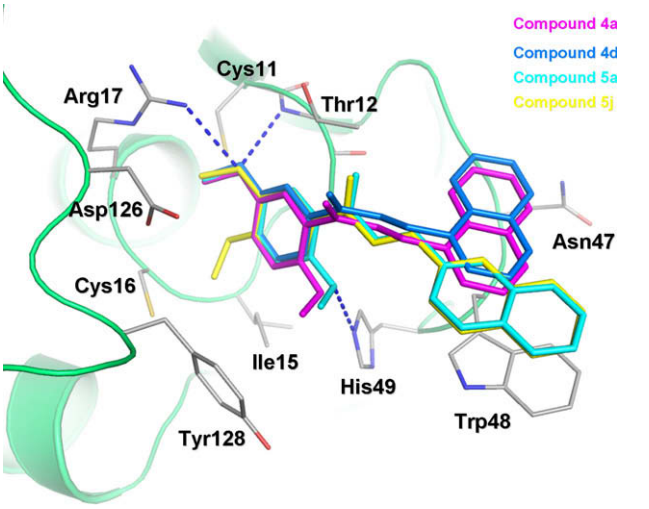

Figure 3. Modeled binding mode of the chalcone analogs within the MPtpA active site. Protein residues involved in ligand binding are indicated as stick model and hydrogen bonds are illustrated as blue dashed lines.

three hydrogen bonds from: (i) the main chain NH of Thr12, (ii) the NH_2 side chain of Arg17, and (iii) the NH_2 side chain of His49 residues of the PtpA binding site. Similarly, the oxygen atom of the *m*-methoxy substituent of **5j** (K_i = 4.9 μM) accepts two hydrogen bonds (Thr12 and Arg17), however, the *p*-methoxy substituent is shown to be directed into a deeper cavity pointing towards the side chain of Cys16 and Ile15 residues. The binding mode of **4d** (K_i = 9.1 μM) also indicates two hydrogen bonds between the *o*-methoxy substituent and Thr12 and Arg17. In addition, the electron-rich 2-naphthyl group (B-ring) of the chalcones **5a** and **5j** undergo π-stacking with the side chain of the Trp48 in a classic parallel-displaced arrangement (Fig. 3). Conversely, this interaction is not efficiently established in the proposed binding mode of **4a** and **4d**, which shows the 1-naphthyl group at this position. The integrated analysis involving the SAR data and the molecular modeling results suggests that the π–π interactions considerably contribute to the observed inhibitory activity, in agreement to Ellman and co-workers data for another inhibitor compound.[17] In fact, the 2-naphthyl derivative **5a** (K_i = 5.4 μM) was approximately fivefold more potent than the 1-naphthyl derivative **4a** (K_i = 21 μM). Successful examples of aromatic ring interactions have been described for a number of important systems for rational drug design and lead optimization in medicinal chemistry.[31–33] Therefore, the binding mode of the chalcones indicates that the *o*,*m*-methoxy substitution patterns of the A-ring, and the 2-naphthyl group as B-ring play important roles in orientating the inhibitors within the active site, as well as significantly contributing to the biological activity observed for these inhibitors.

Besides providing useful insights for the understanding of the SAR data, the modeled binding modes of the inhibitors revealed some structural elements that can be explored to improve both inhibitory potency and selectivity. On this basis, further optimization efforts on these compounds are currently underway. Examples of molecular modifications include: (i) substitution of a hydrophobic group at the *p*-position of A-ring, predicted to interact to the side chain of Cys16 and Ile15; and (ii) replacement of the naphthyl moiety with an electron-rich heterocycle group (e.g., indole, quinoline, quinoxaline).

2.3. Selectivity assay

In general, PTP members share low sequence identity, but the defining consensus sequences, the active site P loop motif – $C(X)_5R(S/T)$– and an essential Asp that functions as a general acid in the catalytic reaction, are conserved.[34,35] While PtpA belongs to the low-molecular-weight (LMW) PTP family,[34] PtpB sequence falls into the conventional PTP or dual-specificity phosphatase (DSP) family.[35] PtpA is 37% identical and presents high structural similarity to the human LMW PTP, but there are significant changes around the active site and the protein tyrosine phosphatase (PTP) loop.[16] To verify the possibility of inhibition of other tyrosine phosphatases we assayed the described chalcones on mycobacterial PtpB and in the human PTP1B.

No inhibition was detected with compounds **5i**, **4d**, **4a**, **5a**, and **5j** at 100 μM when tested in PtpB from Mtb (data not shown). We also assayed PTP1B (human Ptp) with chalcones **5i**, **4d**, **4a**, **5j**, and **5a**, and their IC_{50} were 123.03 μM, 158.49 μM, 213.80 μM, 1258.93 μM, and 144.54 μM, respectively. These assays suggested the selectivity of these compounds towards PtpA from *M. tuberculosis*.

2.4. Inhibitors of MPtpA reduce mycobacterial survival in macrophages

Mtb reside and replicate within human alveolar macrophages. As such candidate drugs need to cross the macrophage membrane barrier in order to inhibit their molecular target with limited cytotoxic effect on the host macrophage. Thus, we examined the effect of the inhibitors on the macrophage cell line THP-1. Table 2 describes the percentage of human derived THP-1 macrophages survival when subjected to the indicated concentration of each inhibitor. The least toxic inhibitors were **4d** and **5j**, which have killed only 2.0 and 1.6% of the cells, respectively, at a 40 μM concentration. Interestingly a direct effect of the chalcones in Mtb growth in vitro was not observed (data not shown), consistent with the recently described MtbPtpB inhibitors.[36]

To further investigate the potential of the chalcones examined in an in vivo assay, we first focused on the effect of the chalcones on the survival of the vaccine strain *Mycobacterium bovis* BCG. As illustrated in Table 3 at 20 μM over 48 h four of the compounds had an effect on the survival rate of this strain in macrophages. The growth of a *ptp*A knockout strain of *M. tuberculosis* in THP-1

Table 2
Toxicity of the five chalcone analog inhibitors in human macrophages

Inhibitor	40 μM (% ± SD)[a]	4 μM (% ± SD)[a]
5i	10.5 ± 0.24	0.9 ± 0.20
4d	2.0 ± 0.21	
4a	77.8 ± 1.5	0.9 ± 0.32
5j	1.6 ± 0.26	
5a	83.1 ± 7.9	1.3 ± 0.41
Negative control	8.1 ± 0.48	1.0 ± 0.30
Positive control	99.7 ± 0.01	25.9 ± 11

[a] Percentage and standard deviation (SD) values of killed THP-1 cells exposed to different concentrations of the inhibitors. The experiments were carried out in triplicates (5000 cells counted by flow cytometry).

Table 3
BCG macrophage infection

Inhibitor	Average (%) 24 h[a]	Average (%) 48 h[b]
5i	72.9	8.5
4d	180.8	71.3
4a	108.6	46.3
5j	63.8	32.9
5a	117.7	234.9

[a] Percentage and standard deviation (SD) values of resistant CFUs exposed to 10 μM of each inhibitor after 24 h.
[b] Percentage and standard deviation (SD) values of resistant CFUs exposed to 20 μM of each inhibitor after 48 h. Assays were carried out in triplicate.

macrophages was shown to be attenuated when compared to the parental H37Rv strain.[10] We hypothesized that chemical inhibition of PtpA would similarly impair the intracellular survival of *M. tuberculosis*. The five chalcones (**5i**, **4d**, **4a**, **5j**, and **5a**) were therefore tested for their ability to reduce *M. tuberculosis* survival during macrophage infection. As shown in Figure 4, individual treatment with the five chalcones shows comparable intracellular mycobacterial growth as the untreated strain at 24 h of infection. At 48 h, in the presence of 20 μM of inhibitors, growth differences can be observed: treatment of macrophages with **4a** leads to 77% reduction in bacterial burden as compared to the untreated (DMSO); **4d** and **5a** also resulted in approximately 50% reduction. However, **5i** and **5j** failed to show significant effect on *M. tuberculosis* growth within THP-1 macrophages at 48 h. Within 96 h, the untreated strain established stable infection as evidenced from the increase in bacterial growth. For the inhibitor treated macrophages, **4a** and **5a** show greater than 90% decrease in bacterial load at 96 h while **4d** leads to 77% reduction. Surprisingly, treatment with **5i** and **5j**, which was ineffective at 48 h, produced greater than 80% and 40% reduction respectively by 96 h. The delayed effect of **5i** and **5j** might be due to differences in the ability to cross macrophage cell membranes. Despite their efficacy in bacterial clearance, toxicity assay shows that **4a** and **5a** also reduces the viability of THP-1 macrophages. Therefore, the observed decrease in bacterial burden might be simply due to macrophage cell death instead of mycobactericidal effect. In this regard, **4d**, which does not show toxicity against human macrophages, would be the most effective inhibitor in reducing the intracellular growth of *M. tuberculosis*. Further efforts are necessary to increase the gap between toxicity toward macrophages and useful antibacterial activity.

2.5. Chalcones inhibit dephosphorylation of the natural substrate of the mycobacterial PtpA

It was shown earlier that the primary target of *M. tuberculosis* PtpA is the host protein kinase VPS33B.[10] Thus an assay with chalcone **4d** was performed to test whether inhibition of PtpA results in decreased dephosphorylation of VPS33B. As shown in Figure 5, a dose-dependent increase in VPS33B phosphorylation can be observed when PtpA is treated with the chalcone inhibitor as compared to the control reaction without inhibitor. This finding indicates that beyond in vitro inhibition of PtpA activity towards an artificial substrate (pNPP), the selected chalcone is capable of acting on the dephosphorylation of a bona fide target of PtpA.

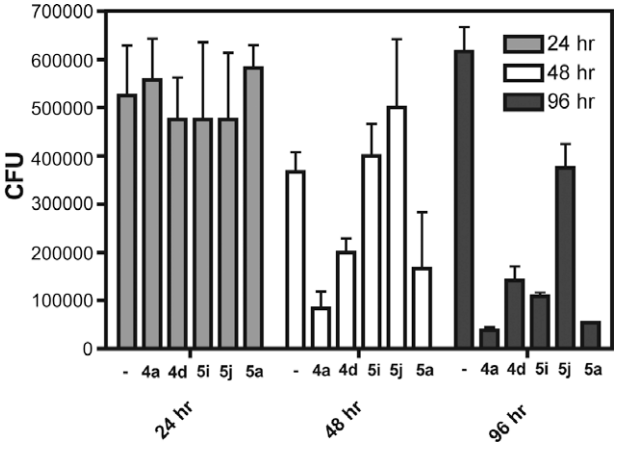

Figure 4. Mtb survival in infected THP-1 macrophages treated with the chalcone inhibitors. Differentiated THP-1 macrophages were infected with the H37Rv Mtb strain and treated with 10 μM of the indicated inhibitor at 0 hr. The second and third doses were added at 24 h and 48 h, respectively. Survival of intracellular Mtb (CFU) was determined by plating on 7H10 agar. DMSO was used as a negative control (−). Data are expressed as mean CFU for triplicate wells with standard deviation values.

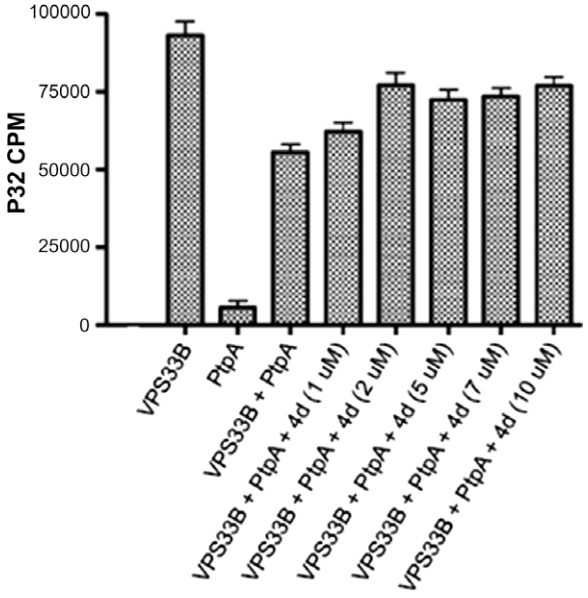

Figure 5. In vitro dose-dependent inhibition of PtpA by the chalcone **4d**. VPS33B (0.44 μM) was incubated with γ^{32}P-ATP for 1 h previous to the addition of different concentrations of the chalcone, **4d**, and the tyrosine phosphatase, PtpA (3.93 μM). Incubation was followed for 15 min and the phosphatase activity was measured in a scintillation counter. Results are expressed as mean ± SD.

3. Conclusions

Enzyme inhibitors, beyond their role in the treatment of the disease might also be useful as probe molecules in chemical biology approaches to dissect the role of PtpA and PtpB phosphatases in host-pathogen invasion. In fact, in this work we clearly demonstrated that inhibition in vitro of PtpA is correlated to in vivo inhibition of mycobacterial survival, and interestingly to diminished dephosphorylation of the natural target of PtpA in macrophages, VPS33B.

These active chalcones are easily obtained with low cost, are rather simple structurally, and may represent a novel lead compounds to be used in strategies to combat tuberculosis.

4. Experimental Section

4.1. Enzyme kinetics

To determine the type of inhibition, inhibitors **5i**, **4d**, **4a**, 5j, and **5a** were selected and screened for each concentration of pNPP (0.5, 1.5, 3, 6, 8, 15, 25 and 40 mM). The phosphatase assays were carried out in 96-well plates containing PtpA buffer (25 mM Tris–HCl pH 8.0, 20 mM imidazole pH 7.0, 40 mM dithiothreitol, 20% glycerol, different concentrations of inhibitors and pNPP) followed by addition of 2 μl of recombinant PtpA (1.0 μg/μl) diluted in PtpA buffer in order to initiate the reaction. The absorbance at 410 nm was measured for 20 min, at 37 °C in an ELISA plate spectrophotometer (TECAN). Negative controls were performed in the absence of enzyme, and positive controls were carried out in the presence of enzyme and DMSO. All assays were done in triplicate.

The phosphate released (Vi) was quantified and analyzed as a Lineweaver–Burk plot ($1/Vi \times 1/[S]$) generated in the SIGMAPLOT Software 9.0. The values of K_i, V_{max}, K_{mapp} for each compound were determined from the collected data by nonlinear regression analysis. To estimate the inhibition constants, a range of pNPP

concentrations was used for each assay with three concentrations for each inhibitor. The Dixon plot was designed by plotting 1/Vi as a function of [*I*], and inhibition constant (K_i) was determined as the intercept of each line (different substrate concentrations) generated in the SigmaPlot Software 9.0. Alternatively, K_{mapp} values obtained for each compound concentration were plotted versus [*I*] with the intercept of the curve and *X*-axis corresponding to $-K_i$.

The assays for selectivity using PtpB and PTP1B were carried out as described.[25]

4.2. Molecular modeling

The 3D structures of the chalcone inhibitors were constructed using standard geometric parameters of the molecular modeling software package SYBYL 8.0. Each single optimized conformation of each molecule in the data set was energetically minimized employing the Tripos force field[37] and the Powell conjugate gradient algorithm[38] with a convergence criterion of 0.05 kcal/mol Å and Gasteiger–Hückel charges.[39]

Molecular docking and scoring protocols as implemented in FlexX[30] (BioSolveIT GmbH, Sankt Augustin—Germany) were used to investigate the possible binding conformations of the ligands within the PtpA binding pocket. The X-ray crystallographic data for PtpA determined at 1.9 Å (PDB ID 1U2P)[34] used in the docking simulations were retrieved from the Protein Data Bank (PDB). The chloride ion and water molecules were removed from the binding pocket. Hydrogen atoms were added in standard geometry using the Biopolymer module implemented in SYBYL 8.0. Histidines, glutamines, and asparagines residues within the binding site were manually checked for possible flipped orientation, protonation, and tautomeric states with Pymol 0.99 (DeLano Scientific, San Carlos, USA) side chain wizard script. The binding site was defined as all the amino acid residues encompassed within a 10 Å radius sphere centered on the three dimensional coordinates of the chloride ion bound to the active site. The docking procedures were repeated 30 times for each inhibitor. The implemented FlexX scoring function and visual inspection were employed to select the representative conformation for each inhibitor.

4.3. Toxicity assay

The toxicity characteristics of the compounds were determined using FACS analysis as described previously.[40]

4.4. VPS33B phosphorylation assay

VPS33B (0.44 μM) was incubated with γ^{32}P-ATP and kinase buffer (0.5 M Tris–HCl pH 8.0, 0.025 M MnCl, 0.05 M MgCl, 0.1 M DTT) for 1 h at 37 °C to allow autophosphorylation to occur. PtpA (3.93 μM) and different concentrations of chalcone **4d** (1 μM, 2 μM, 5 μM, 7 μM and 10 μM) were then added to VPS33B and incubation at 37 °C was continued for 15 min. Reactions were stopped by spotting 10 μl of each reaction mixture onto a Whatman paper. Dried papers were washed six times for 10 min each in 1% phosphoric acid. The papers were loaded into vials and the kinase activity of VPS33B was measured in a scintillation counter. Results are expressed as mean ± SD.

4.5. Cell and bacterial culture conditions and macrophage infections

THP-1 monocytes [41] were cultured in RPMI-1640 (Sigma®) supplemented with 10% heat inactivated fetal bovine serum (FBS), 1% L-glutamine, and 1% Penicillin–Streptomycin at 37 °C with 5% CO_2. *M. tuberculosis* H37Rv was grown in Middlebrook 7H9 (Difco) containing 0.05% Tween-80 and 10% oleic acid/albumin/dextrose/catalase (OADC) enrichment at 37 °C. For the induction of THP-1 macrophage differentiation, cells were seeded in 12-well tissue culture plates (Corning) at 7×10^5 cells per well in RPMI-1640 (supplemented with 10% FBS and 1% L-glutamine) with 80 ng/μl phorbol myristate acetate (PMA) for 24 h at 37 °C with 5% CO_2. The differentiated cells were then washed three times with RPMI-1640 to remove non-adherent cells. Bacteria was opsonized with human serum before infection, and infection of THP-1 macrophages was performed at a multiplicity of infection (MOI) of 10:1 (Bacteria/macrophage) for 3 h at 37 °C with 5% CO_2. Infected macrophages were washed three times with RPMI-1640 to remove extracellular bacteria and replaced with 1 mL fresh RPMI medium (supplemented with 10% FBS, 1% L-glutamine and 100 μg/mL Gentamicin) with the appropriate PtpA inhibitor at a concentration of 10 μM. This is then defined as time 0 h. A second and third dose of inhibitors were added at 24 h and 48 h, respectively. At defined time points, the infected macrophages were lysed with 0.025% SDS, and the number of viable bacteria was determined by plating serial dilutions of each well on Middlebrook 7H10 Agar supplement with 10% OADC. The plates were incubated at 37 °C for 21 days before counting was performed. All experiments were performed in triplicates.

Acknowledgments

We would like to thank the Departmentos de Química and Bioquímica—Universidade Federal de Santa Catarina and the Instituto de Física de São Carlos—Universidade de São Paulo, Brazil, for the use of equipments and some facilities. We thank CNPq, CAPES, FAPESC, FAPESP, MCT and FINEP for financial support.

Supplementary data

Supplementary data associated with this article can be found, in the online version, at doi:10.1016/j.bmc.2010.04.051.

References and notes

1. Maher, D.; Raviglione, M. *Clin. Chest Med.* **2005**, *26*, 167.
2. Gelperina, S.; Kisich, K.; Iseman, M. D. *Am. J. Respir. Crit. Care Med.* **2005**, *172*, 1487.
3. Ruiz-Manzano, J.; Blanquer, R.; Calpe, J. L.; Caminero, J. A.; Caylà, J.; Domínguez, J. A.; García, J. M.; Vidal, R. *Arch. Bronconeumol.* **2008**, *44*, 551.
4. Balganesh, T. S.; Alzari, P. M.; Cole, S. T. *Trends Pharmacol. Sci.* **2008**, *29*, 576.
5. Cole, S. T.; Brosch, R.; Parkhill, J.; Garnier, T.; Churcher, C.; Harris, D.; Gordon, S. V.; Eiglmeier, K.; Gas, S.; Barry, C. E.; Tekaia, F.; Badcock, K.; Basham, D.; Brown, D.; Chillingworth, T.; Connor, R.; Davies, R.; Devlin, K.; Feltwell, T.; Gentles, S.; Hamlin, N.; Holroid, S.; Hornsby, T.; Jagels, K.; Krogh, A.; McLean, J.; Moule, S.; Murphy, L.; Oliver, K.; Osborne, J.; Quail, M. A.; Rajandream, M. A.; Rogers, J.; Rutter, S.; Seeger, K.; Skelton, J.; Squares, R.; Squares, S.; Sulston, J. E.; Taylor, K.; Whitehead, S.; Barrell, B. G. *Nature* **1998**, *393*, 537.
6. Hestvik, A. L.; Hmama, Z.; Av-Gay, Y. *Infect. Immunol.* **2003**, *71*, 5514.
7. Koul, A.; Herget, T.; Klebl, B.; Ullrich, A. *Nat. Rev. Microbiol.* **2004**, *2*, 189.
8. Chao, J.; Wong, D.; Zheng, X.; Poirier, V.; Bach, H.; Hmama, Z.; Av-Gay, Y. *Biochim. Biophys. Acta*, in press.
9. Koul, A.; Choidas, A.; Treder, M.; Tyagi, A. K.; Drlica, K.; Singh, Y.; Ullrich, A. *J. Bacteriol.* **2000**, *182*, 5425.
10. Bach, H.; Papavinasasundaram, K. G.; Wong, D.; Hmama, Z.; Av-Gay, Y. *Cell Host Microbe.* **2008**, *3*, 316.
11. Bach, H.; Wong, D.; Av-Gay, Y. *Biochem. J.* **2009**, *420*, 155.
12. Tautz, L.; Bruckner, S.; Sareth, S.; Alonso, A.; Bogetz, J.; Bottini, N.; Pellecchia, M.; Mustelin, T. *J. Biol. Chem.* **2005**, *280*, 9400.
13. Bialy, L.; Waldmann, H. *Angew. Chem., Int. Ed.* **2005**, *44*, 2.
14. Manger, M.; Scheck, M.; Prinz, H.; von Kries, J. P.; Langer, T.; Saxena, K.; Schwalbe, H.; Fürstner, A.; RAdemann, J.; Waldmann, H. *ChemBioChem* **2005**, *6*, 1749.
15. Vintonyak, V. V.; Antonchick, A. P.; Rauh, D.; Waldmann, H. *Curr. Opin. Chem. Biol.* **2009**, *13*, 272.
16. Madhurantakam, C.; Chavali, V. R. M.; Das, A. K. *Proteins* **2008**, *71*, 706.
17. Rawls, K. A.; Lang, P. T.; Takeuchi, J.; Imamura, S.; Baguley, T. D.; Grundner, C.; Alber, T.; Ellman, J. A. *Bioorg. Med. Chem.* **2009**, *19*, 6851.
18. Koch, M. A.; Waldmann, H. *Drug Discovery Today* **2005**, *10*, 471.

19. Grundner, C.; Perrin, D.; Hooft van Huijsduijnen, R.; Swinnen, D.; Gonzalez, J.; Gee, C. L.; Wells, T. N.; Alber, T. *Structure* **2007**, *15*, 499.
20. Corrêa, I. R., Jr.; Nören-Müller, A.; Ambrosi, H.; Jakupovic, S.; Saxena, K.; Schwalbe, H.; Kaiser, M.; Waldmann, H. *Chem. Asian J.* **2007**, *2*, 1109.
21. Koch, M. A.; Wittenberg, L. O.; Basu, S.; Jeyaraj, D. A.; Gourzoulidou, E.; Reinecke, K.; Odermatt, A.; Waldmann, H. *Proc. Natl. Acad. Sci. U.S.A.* **2004**, *101*, 16721.
22. Forghieri, M.; Laggner, C.; Paoli, P.; Langer, T.; Manao, G.; Camici, G.; Bondioli, L.; Prati, F.; Constantino, L. *Bioorg. Med. Chem.* **2009**, *17*, 2658.
23. Westbrook, J.; Feng, Z.; Chen, L.; Yang, H.; Berman, H. M. *Nucleic Acids Res.* **2003**, *31*, 489.
24. Moitessier, N.; Englebienne, O.; Lee, D.; Lawandi, J.; Corbeil, C. R. *Br. J. Pharmacol.* **2003**, *153*, S7.
25. Chiaradia, L. D.; Mascarello, A.; Purificação, M.; Vernal, J.; Cordeiro, M. N. S.; Zenteno, M. E.; Villarino, A.; Nunes, R. J.; Yunes, R. A.; Terenzi, H. *Bioorg. Med. Chem. Lett.* **2008**, *18*, 6227.
26. Dimmock, J. R.; Elias, D. W.; Beazely, M. A.; Kandepu, N. M. *Curr. Med. Chem.* **1999**, *6*, 1125.
27. Ni, L.; Meng, Q. C.; Sikorski, J. A. *Expert Opin. Ther. Patents* **2004**, *14*, 1669.
28. (a) Lin, Y. M.; Zhou, Y.; Flavin, M. T.; Zhou, L. M.; Nie, W.; Fa-Ching, C. *Bioorg. Med. Chem.* **2002**, *10*, 2795; (b) Yoon, G.; Lee, W.; Kim, S. N.; Cheon, S. H. *Bioorg. Med. Chem. Lett.* **2009**, *19*, 5155; (c) Hans, R. H.; Guantai, E. M.; Lategan, C.; Smith, P. J.; Wanc, B.; Franzblau, S. G.; Gut, J.; Rosenthal, P. J.; Chibale, K. *Bioorg. Med. Chem. Lett.* **2010**, *20*, 942.
29. Copeland, R. A. Reversible Modes of Inhibitor Interactions with Enzymes. In *Evaluation of Enzyme Inhibitors in Drug Discovery*; Wiley Interscience: New Jersey, 2005; pp 48–81.
30. Rarey, M.; Kramer, B.; Lengauer, T.; Klebe, G. *J. Mol. Biol.* **1996**, *261*, 470.
31. Meyer, E. A.; Castellano, R. K.; Diederich, F. *Angew. Chem., Int. Ed.* **2003**, *42*, 1210.
32. Mitchell, J. B.; Nandi, C. L.; McDonald, I. K.; Thornton, J. M.; Price, S. L. *J. Mol. Biol.* **1994**, *239*, 315.
33. McGaughey, G. B.; Gagné, M.; Rappé, A. K. *J. Biol. Chem.* **1998**, *273*, 15458.
34. Madhurantakam, C.; Rajakumara, E.; Mazumdar, P. A.; Saha, B.; Mitra, D.; Wiker, H. G.; Sankaranarayanan, R.; Das, K. *J. Bacteriol.* **2005**, *187*, 2175.
35. Grundner, C.; Ng, H. L.; Alber, T. *Structure* **2005**, *13*, 1625.
36. Beresford, N. J.; Mulhearn, D.; Szczepankiewicz, B.; Liu, G.; Johnson, M. E.; Fordham-Skelton, A.; Abad-Zapatero, C.; Cavet, J. S.; Tabernero, L. *J. Antimicrob. Chemother.* **2009**, *63*, 928.
37. Clark, M.; Cramer, R. D.; van Opdenbosch, N. *J. Comput. Chem.* **1989**, *10*, 982.
38. Powell, M. J. D. *Math. Program* **1977**, *12*, 241.
39. Gasteiger, J.; Marsili, M. *Tetrahedron* **1980**, *36*, 3219.
40. Pick, N.; Cameron, S.; Arad, D.; Av-Gay, Y. *Biol. Proced. Online* **2004**, *6*, 220.

Please cite this article in press as: Mascarello, A.; et al. *Bioorg. Med. Chem.* (2010), doi:10.1016/j.bmc.2010.04.051